Gas-Phase Vanadium Oxide Anions: Structure and Detachment Energies from Density Functional Calculations

Sergei F. Vyboishchikov and Joachim Sauer*

Humboldt-Universität zu Berlin, Institut für Chemie Arbeitsgruppe Quantenchemie, Jägerstrasse 10-11, D-10117 Berlin, Germany

Received: May 26, 2000; In Final Form: September 6, 2000

Mononuclear and binuclear vanadium oxide anions, VO_y^- ($y = 1-4$) and $V_2O_y^-$ ($y = 4$, 6, and 7), as well as the polynuclear $V_3O_8^-$, $V_4O_{10}^-$, and $V_4O_{11}^-$ anions are examined using density functional methods. Comparison is made with the corresponding neutral systems, and the vertical detachment energies of the anions and the adiabatic electron affinities of the neutrals are calculated. A triple-ζ valence plus polarization basis set is adopted and the B3LYP and BP86 functionals are employed. The two functionals yield very similar structures for all systems studied. The electron detachment energies of the anions display two important trends. First, they increase strongly with increasing metal oxidation state. Second, the electron detachment energies increase with a higher delocalization of the unpaired electron of the anion. The electron detachment energies of peroxo complexes are not higher than those of analogous complexes without an O_2 ligand. Energies for oxygen uptake decrease with increasing oxygen-to-vanadium ratio. They are particularly low when a peroxo group is formed. Formation of larger species from smaller ones is energetically favorable. The $V_3O_8^-$ ion appears to be particularly stable.

1. Introduction

Transition metal oxides are important to both organic and inorganic chemistry, mainly due to their ability to catalyze various oxidation reactions. Solid divanadium pentaoxide plays a special role because it effects a broad range of reactions, from $SO_2 \rightarrow SO_3$ oxidation to oxidative dehydrogenation of alkanes.[1−3] Although solid materials are predominantly employed in industrial catalytic processes, small metal oxide clusters also attract attention as potentially active species. Substantial work in this area has been carried out by A. W. Castleman Jr. and co-workers.[4−7] Cationic metal oxide clusters are generated directly from metal and oxygen under plasma conditions and subsequently separated by mass spectrometry. Reactions of various $V_xO_y^+$ ions with several organic substrates were reported. The most stable cations correspond to the $(VO_2)_n(V_2O_5)_m(O_2)_q^+$ composition. The O_2 units were shown to be only weakly bound to the $(VO_2)_n(V_2O_5)_m$ moiety. Ab initio calculations at modest level provided some idea about the structure of the cations. Small cationic species such as VO_2^+ and their reaction with hydrocarbons were examined by Schwarz and co-workers.[8]

Neutral V_xO_y clusters and their growth dynamics were examined by Foltin et al.[9] They obtained clusters of composition $(VO)_n(VO_2)_m$ as well as oxygen-poorer species. The study showed that the clusters grow only by uptake of VO or VO_2.

Anionic $V_xO_y^-$ species were also studied. Rudnyi et al. detected the VO_2^-, VO_3^-, $V_2O_5^-$, $V_3O_8^-$, and $V_4O_{10}^-$ anions in vanadium oxide vapor at high temperature.[10] The authors estimated equilibrium constants of several reactions of these species and were able to determine their enthalpies of formation as well as electron affinities for VO_2 and V_4O_{10}. The same ions as well as $V_3O_7^-$ were obtained later by Dinca *et al.*[11] They showed decreasing reactivity with increasing size in reactions with various esters. Wu and Wang[12] studied the VO_y^- ($y = 1-4$) anions by photoelectron spectroscopy. The corresponding neutral particles were thoroughly examined by Knight *et al.*[13] both experimentally by EPR and quantum chemically using Hartree−Fock, CAS SCF, and multireference configuration interaction methods. Very recently, $V_xO_y^-$ ions with $x > 1$ were detected by Pramann and Rademann.[14] In most cases, oxygen-rich species were found with a formal vanadium oxidation state slightly below or even above 5. Hartree−Fock and DFT calculations for fixed structures on the Lundqvist anions $V_{10}O_{28}^{6-}$ and $V_{12}O_{32}^{4-}$ have been reported by Bénard and co-workers.[15−17] Their research was mainly focused on predicting nucleophilic behavior of the anions using electrostatic potential distribution, and on guest−host interaction.

For other metals (Cu, Fe, Al), O-excess clusters have been examined by photoelectron spectroscopy.[18−20] Gutsev et al.[21] made DF calculation on mononuclear iron oxide anions FeO_x^-. For the electron affinities, reasonable agreement with the experimental values was achieved. As expected, in the FeO_x^- series the electron affinities increase with increasing x. Oxygen-rich anions were found to be quite stable with respect to their neutral parents even if the latter have closed electron shells.

Our interest is to determine the structure of $V_xO_y^-$ anions and their vertical electron detachment energies (VDE) by density functional (DF) techniques.[22] We will also calculate adiabatic electron affinities, which requires a determination of the equilibrium structures of the respective neutral species.

2. Computational Methods

The present study employs two different density functionals: (1) a hybrid functional including Becke's 1988 nonlocal exchange functional[23] as well as Hartree−Fock exchange along with the Lee−Yang−Parr[24] correlation functional (**B3LYP**),[25,26]

* To whom correspondence should be addressed. Tel: +49-30-20192300. Fax: +49-30-20192302. E-mail: js@qc.ag-berlin.mpg.de.

10.1021/jp001936x CCC: $19.00
Published on Web 10/21/2000

TABLE 1: Comparison of Experimental and Calculated (TZVP basis set) Atomization Energies (kJ/mol) and Structural Parameters (Å, Degrees) for Selected Vanadium Molecules

molecule	atomization energy			structure[a]			
	experiment (D_0)	B3LYP (D_e)	BP86 (D_e)	parameter	experiment	B3LYP	BP86
^{5}VH	159 ± 13[b] 172 ± 17[c]	171	186	V−H	1.719	1.693	1.684
$^4VH^+$	198 ± 6[d] 209 ± 8[e]	225	231	V−H		1.637	1.628
^{4}VO	625 ± 19[f] 625 ± 9[g]	509	610	V−O	1.589[h] 1.592[i]	1.590 1.580[j]	1.596
$^2VO_2$	1177 ± 18[g]	1017	1209	V−O O−V−O	1.589 110°	1.616 114.4°	1.618 109.5°
$VOCl_3$	1800[h]	1569	1795	V−O V−Cl Cl−V−Cl	1.570 2.142 111.3°	1.561 2.154 110.8°	1.579 2.157 110.8°
VOF_3	2240[h]	2005	2250	V−O V−F F−V−F	1.570 1.729 111.2°	1.561 1.732 110.6°	1.580 1.740 110.8°

[a] Ref 38 [b] Ref 39 [c] Ref 40 [d] Ref 41 [e] Ref 42 [f] Ref 43 [g] Ref 44 [h] Ref 45 [i] Ref 46 [j] Ref 60

and (2) Becke's exchange functional[23] in combination with Perdew's correlation functional (**BP86**).[27] For open-shell systems, spin-unrestricted, otherwise restricted Kohn−Sham equations are solved.

For transition metal complexes, the B3LYP method yields accurate structures and, in many cases, also reasonable relative energies.[28] As far as the performance for anions is concerned, the only systematic study is the calculation of electron affinities for the so-called G-2 set of molecules,[29] which does not include transition metal compounds. B3LYP performs rather well for ionization potentials (average deviation is 0.177 eV), and the performance for electron affinities is even better (average deviation is 0.131 eV). The BP86 functional is generally less reliable but permits substantial savings of computation time when the RI-DFT ("resolution of identity") procedure[30] is applied. For the species under study, BP86 using the RI-DFT is 5 to 7 times faster than B3LYP with the TURBOMOLE program.[31] Comparison for neutral closed-shell $(V_2O_5)_n$ clusters shows that B3LYP and BP86 yield very similar structures and energies.[32]

The calculations were performed with an all-electron triple-ζ valence basis set (TZV) optimized by Ahlrichs and co-workers [33,34] and augmented by a set of polarization functions (a *p*-function for vanadium, a *d*-function for oxygen) (TZVP basis set). The contraction scheme for the {s/p/d} functions is {842111/6311/411} for vanadium and {62111/411/1} for oxygen. Although the outermost exponents of this basis set are small (0.035 for vanadium, 0.175 for oxygen), it should be noted that diffuse basis functions may be needed to correctly describe anionic species. The influence of diffuse functions is considered in detail in Section 4.4.

To estimate the electron coupling of two electrons at two centers, which is present in V_2O_4, we used the "broken-symmetry" approach.[35,36] In this method, the open-shell singlet−triplet energy splitting $E_S - E_T$ is approximated by the formula

$$E_S - E_T \approx \frac{2(E_{BS} - E_T)}{2 - \langle \hat{S}^2 \rangle_{BS}}$$

where $\langle \hat{S}^2 \rangle_{BS}$ is the expectation value of the $\hat{S}^2$ operator for the unrestricted broken-symmetry wave function; E_S, E_T, E_{BS} have the energies of the open-shell singlet, $\{\varphi_1\bar{\varphi}_2\} - \{\varphi_2\bar{\varphi}_1\}$, of the triplet $\{\varphi_1\varphi_2\}$, and of the single-determinant broken-symmetry solution, $\{\varphi_1\bar{\varphi}_2\}$, respectively.

The structures of the anions were optimized. To determine VDE of the anions, single-point calculations of the respective neutral species at the anion structure were carried out. The structures of the neutral species were also optimized. All geometry optimizations and single-point calculations were performed with the TURBOMOLE program package.[31] To characterize the stationary points found by optimization, harmonic force constants were calculated analytically at the BP86/TZVP level using the Gaussian 94 package.[37]

3. Performance of DF Calculations

To test the performance of the computational method chosen, we carried out calculations on small vanadium-containing molecules, for which experimental gas-phase data are available for structures and energies. These molecules make up a subset of species that were used by Jug et al. for fitting parameters for the semiempirical SINDO1 method.[38] Table 1 shows the results of these calculations.

The comparison between the experimental and calculated values indicates that B3LYP/TZVP underestimates atomization energies, with the exception of VH and VH^+. The BP86/TZVP results are in excellent agreement with the experiment. Except for VH^+ and VO_2, the deviation is within the range of experimental uncertainty. The calculated structures show a very good agreement for both functionals. Bond distances differ only by at most 0.03 Å, B3LYP doing slightly better. For B3LYP bond angles, however, there is a deviation for VO_2, which is not present in the BP86 result.

Excitation energies of the anions, albeit out of the scope of the present work, also provide a basis for comparison with available experimental data and additional evaluation of the quality of the DF calculations. Few experimental data are available for the anions of interest in the present study. For VO, the second lowest state is $^2\Sigma^-$. It lies 0.554 eV (B3LYP) or 0.676 eV (BP86) above the quartet ground state, in good agreement with the photoelectron data (0.70 ± 0.01 eV).[12] For VO_2^-, it was concluded from the photoelectron spectrum[12] that the lowest excitation energy is about 0.31 eV, in surprising agreement with the BP86 result of 0.33 eV (see the detailed discussion of VO_2^- below in Section 4.1). However, it was not clear from the experiment to which electronic state it should be assigned. The B3LYP excitation energy is almost twice as large as the BP86 result.

4. Results

4.1. Anions with a Partially Occupied Vanadium *d*-Shell. Figures 1−5 show the structures obtained for the vanadium oxide anions and for the corresponding neutral systems.

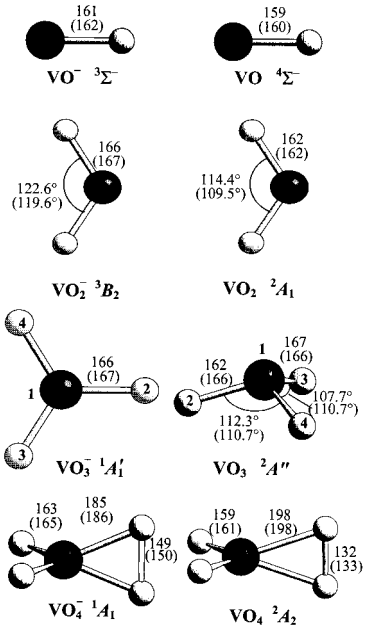

Figure 1. Structures of the VO_y^- ($y = 1-4$) ions and the corresponding neutral species. Vanadium atoms are shown black, oxygen atoms are white. B3LYP distances are given in picometers. (BP86 results in parentheses.)

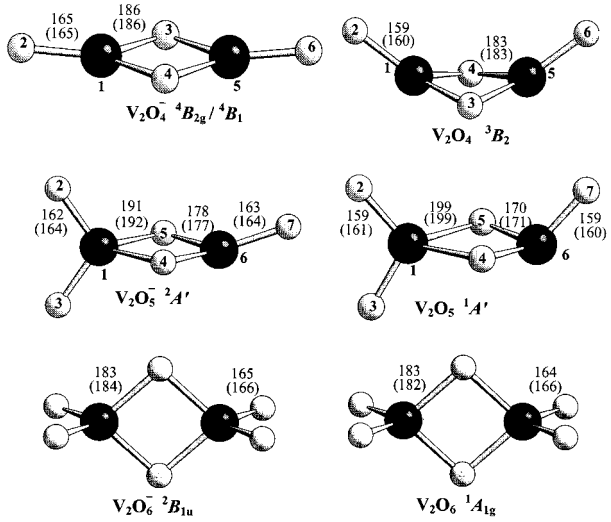

Figure 2. Structures of the dinuclear $V_2O_y^-$ ($y = 4-6$) ions and the corresponding neutral species. Notations are the same as in Figure 1.

VO⁻ and VO. The electronic structure of the neutral VO molecule has been examined extensively by both spectroscopic[45,48−52] and theoretical[13,53−59] methods. Its ground state is a $^4\Sigma^-$ quartet with a $\sigma^2\pi^4\sigma^1\delta^2$ electron configuration. Previously published DF calculations yielded V−O distances of 1.58 Å,[57] 1.61 Å,[57] or 1.60 Å.[59] Our calculations yielded 1.590 and 1.596 Å for the B3LYP and BP86 functionals, respectively, in excellent agreement both with the experimental results of 1.592 Å[50] and 1.589 Å,[45] and with a CAS SCF result of 1.594 Å.[13]

Less is known about the VO^- ion. Using spectroscopic and qualitative MO arguments, Wu and Wang[12] concluded that its ground state is $^5\Pi$ with a $\sigma^2\pi^4\sigma^1\delta^2\pi^1$ electron configuration. According to our DF calculations, however, a triplet $^3\Sigma^-$ state with a $\sigma^2\pi^4\sigma^2\delta^2$ configuration is by 1.18 eV (B3LYP) or 1.13 eV (BP86) more stable than the quintet. The higher stability of the low-spin state is in agreement with the DF calculations of Gutsev et al.[38]

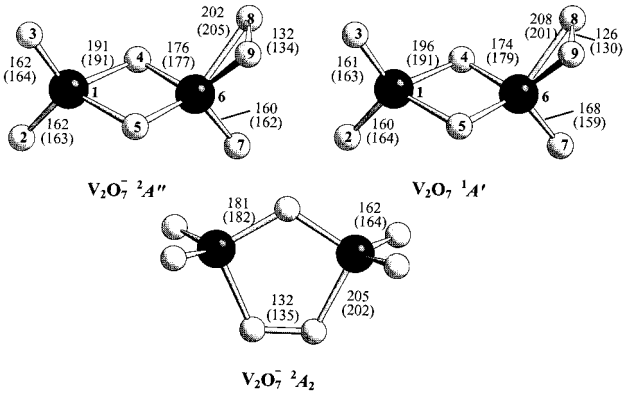

Figure 3. Structures of the $V_2O_7^-$ ion and the neutral V_2O_7. Notations are the same as in Figure 1.

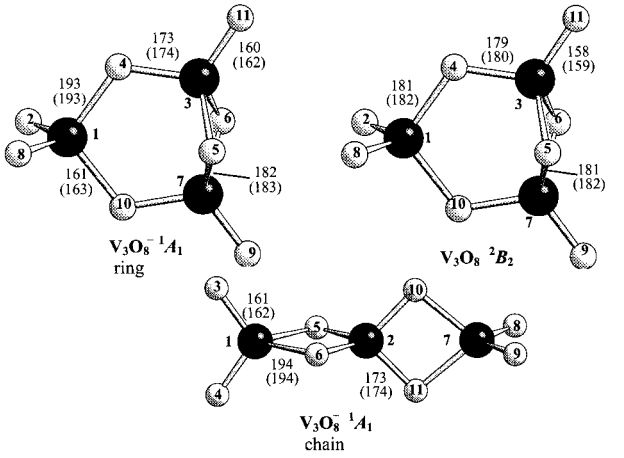

Figure 4. Structures of the $V_3O_8^-$ ion and the neutral V_3O_8. Notations are the same as in Figure 1.

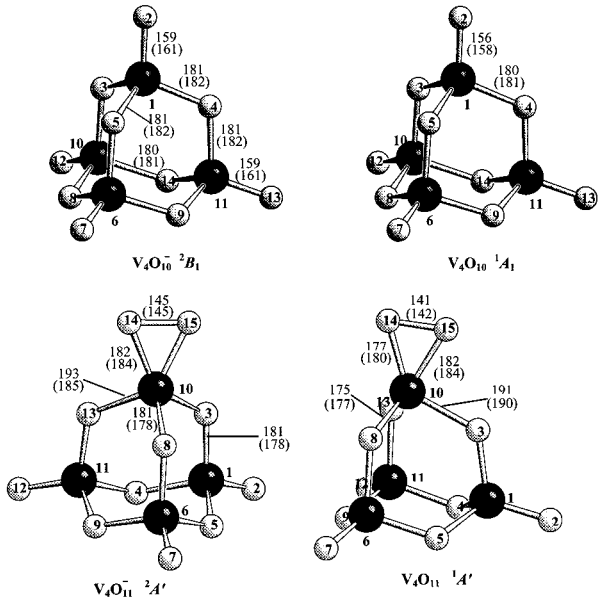

Figure 5. (*a*) Structures of the $V_4O_{10}^-$ ion and the neutral V_4O_{10}. (*b*) Structures of the $V_4O_{11}^-$ ion and the neutral V_4O_{11}. Notations are the same as in Figure 1.

VO_2^- and VO_2. If the neutral VO_2 were linear, the unpaired electron could occupy one of two degenerate nonbonding *d*-orbitals of vanadium (d_{xy} and $d_{x^2-y^2}$, if *z* is the molecular axis), leading to a $^2\Delta_g$ ground state. In the case of a bent (C_{2v}) molecule, this state splits into $^2A_1$ and $^2B_2$. Both B3LYP and BP86 calculations give a bent structure and $^2A_1$ as the ground

state. This is consistent with CAS SCF and MR CI results of Knight et al.[13] as well as with the DF calculations of Harvey et al.[8] The B3LYP and BP86 V−O bond lengths are very similar to each other (see Figure 1), but slightly shorter than the CAS SCF values (1.653 Å).[13] Our predicted O−V−O angles are close to the CAS SCF result (110.5°). The harmonic asymmetric (B_1) V−O stretching vibrational frequency for the neutral VO_2 is 988 cm^{-1} (BP86) which agrees well with the experimental values of 970 cm^{-1} (from vibrational progression of the photoelectron spectrum[12]), and of 943 cm^{-1} (infrared matrix measurements[61]).

Different $^2A_1$ and $^2B_2$ energy splittings are predicted by the B3LYP (0.06 eV) and BP86 (0.24 eV) functionals. High-level ab initio calculations (MR−CISD)[13] predicted the $^2A_1-{}^2B_2$ splitting to be about 0.3 eV. Estimates from EPR spectra gave about 1 eV,[13] whereas photoelectron measurements[12] yielded a value of 0.6 eV. The BP86 result is close to the MR−CISD one, while B3LYP seems to underestimate the $^2A_1-{}^2B_2$ splitting in VO_2.

In view of the electronic structure of the neutral VO_2 and taking into account a relatively small $^2A_1-{}^2B_2$ gap, the triplet $^3B_2$ state (a_1b_2 configuration) is a likely ground state for the VO_2^- ion. Low-lying singlet states of $^1A_1$ symmetry can have either an a_1^2 or b_2^2 configuration, or a mixture of both. An open-shell $^1B_2$ state which stems from the negative linear combination of the $\bar{a}_1b_2$ and $a_1\bar{b}_2$ configurations, is expected to be higher in energy than the triplet state and is not considered here. As expected, the DF calculations gave $^3B_2$ as the ground state, with the $^1A_1$ singlet state by 0.61 and 0.33 eV less stable for the B3LYP and BP86 functionals, respectively. The BP86 value is very close to the experiment (0.31 eV, see Section 3). The structure of VO_2^- is similar to that of neutral species (Figure 1). The V−O bonds are slightly longer in the ion, which can be attributed to a slightly antibonding character of the singly occupied b_2 orbital.

$V_2O_4^-$ and V_2O_4. For V_2O_4, three different structures have been considered, O_2V-VO_2, $O_2V-O-VO$, and $OV-(O)_2-VO$. The latter, which contains a four-membered V−O−V−O ring (Figure 2), was calculated to be much more stable than the others. Because vanadium is in the oxidation state IV (d^1 configuration) and the interaction between the *d*-electrons of the two metal atoms is obviously small, the ground state of the neutral V_2O_4 could be a triplet or an open-shell singlet (ferromagnetic and anti-ferromagnetic coupling, respectively).

The optimized structure of the triplet state of V_2O_4 has C_{2v} symmetry. The V−O−V−O ring is slightly nonplanar, whereas both terminal oxygen atoms are above the ring (cis conformation). For trans conformation, no minimum could be found. The singly occupied MOs consist of metal *d*-orbitals. The lower SOMO (a_1) is a bonding combination of the metal d_{z^2} orbitals (The *z*-axis lies perpendicular to the V−O−V−O ring). The higher SOMO is the antibonding combination of either the d_{z^2} orbitals (b_2) or the $d_{z^2-y^2}$ orbitals (a_2). Consequently, two triplet states can be important for the V_2O_4 molecule: $^3B_2$ and $^3A_2$. The two functionals predict different relative stabilities of these states. According to the B3LYP calculation, the $^3B_2$ state is 0.58 eV lower than $^3A_2$. In contrast, BP86 gives the $^3A_2$ as the ground state, with the $^3B_2$ lying just 0.04 eV above. Another possibility of coupling two electrons at two centers is an open-shell singlet. Because it is an intrinsically multi-configurational (at least two-configurational) system and cannot be properly described by conventional DFT, the "broken-symmetry" approach was applied to the open-shell singlet states $^1A_2$ and $^1B_2$ at fixed geometry of the respective triplet states. Both B3LYP and BP86 calculations indicate that the open-shell singlet of A_2 symmetry is about 0.4 eV less stable than the $^3A_2$ state, whereas the $^1B_2$ state is much higher in energy. This fits to the ab initio result that the binuclear (d^2,d^2) complex $[(NH_3)_5V-O-V(NH_3)_5]^{4+}$ has a high-spin (quintet) ground state.[62]

SCHEME 1

SOMO a_u of $V_2O_4^-$

SOMO a_g of $V_2O_4^-$

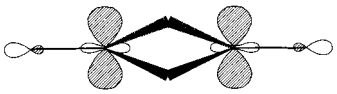

SOMO b_{2u} of $V_2O_4^-$

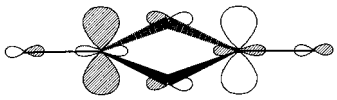

The relevant configurations of the $V_2O_4^-$ ion can be easily derived from the electronic structure of the neutral V_2O_4 molecule. By adding one electron to the $(a_1)^1(b_2)^1$ or $(a_1)^1(a_2)^1$ configurations, a $^2B_2$ ($(a_1)^2(b_2)^1$) or a $^2A_2$ ($(a_1)^2(a_2)^1$) state is obtained, respectively. There is also the possibility of another low-spin state, $^2A_1$, whose configuration can be either $(b_2)^2(a_1)^1$ or $(a_2)^2(a_1)^1$, or a combination of both. As for the neutral V_2O_4, the high-spin $^4B_1$ state of the anion with the $(a_1)^1(a_2)^1(b_2)^1$ configuration is more stable than the low-spin $^2B_2$ and $^2A_2$ states.

The resulting structure of the quartet $V_2O_4^-$ ion is virtually planar. The B3LYP calculation yields an exactly planar geometry of D_{2h} symmetry and a $^4B_{2g}$ state with an $(a_u)^1(a_g)^1(b_{2u})^1$ configuration (Scheme 1).

The BP86 functional predicts a slightly nonplanar cis structure. The deviation of the terminal oxygen atoms from planarity, measured by the V1−V5−O6 angle, is about 5°. The electronic state of this C_{2v} structure is $^4B_1$ ($(a_2)^1(a_1)^1(b_2)^1$ configuration) and corresponds to the $^4B_{2g}$ state of the D_{2h} structure described above.

$V_2O_5^-$ and V_2O_5. For the neutral divanadium pentaoxide molecule (d^0 configuration of V), various oxygen-bridged structures have been considered. The doubly bridged structure $V(O)_2-(O)_2-VO$ and the singly bridged $V(O)_2-O-V(O)_2$ are the most likely candidates for the global minimum. According to our DF calculation, the doubly bridged structure (Figure 2) is 69 and 78 kJ/mol (using the B3LYP and BP86 functionals, respectively) more stable than the singly bridged one. The triply bridged species $V(O)-(O)_3-VO$ is a higher-order saddle point on the potential energy surface and is energetically very high; its optimization without symmetry constraints lead to the doubly bridged structure. In the $V(O)_2-(O)_2-VO$ molecule (C_s symmetry) the V1 and V6 atoms have a tetrahedral and trigonal-pyramidal coordination, respectively. The $V-O^{terminal}$ bonds lengths of about 1.6 Å are typical of V═O double bonds. The $V1-O^{bridge}$ bonds are much longer than the $V6-O^{bridge}$ bonds (Figure 2).

The corresponding anion, $V_2O_5^-$, has a similar doubly bridged structure in its $^2A'$ ground state. The unpaired electron occupies an a' orbital that consists predominantly of the d_{z^2} orbital of the V6 atom (the *z*-axis lies roughly perpendicular to the O4−

SCHEME 2

SOMO a' of $V_2O_5^-$

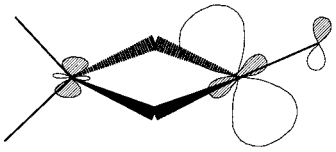

O5−V6 plane) as shown in Scheme 2 and has only very small contributions from a V1 *d*-orbital and from oxygen *p*-orbitals.

In accord with this picture, the Mulliken-type population analysis indicates that virtually all the spin density is accumulated at the V6 atom. Therefore, electron withdrawal from $V_2O_5^-$ corresponds to a $(d^0,d^1) \rightarrow (d^0,d^0)$ transition. The lowest $^2A''$ state of $V_2O_5^-$ is 0.62 eV (B3LYP) and 0.81 eV (BP86) above the ground state. From the structural viewpoint, the main difference between the ground-state $V_2O_5^-$ and the neutral species is that in the anion the V6−O bonds are substantially elongated and the V1−O4/5 bonds are shortened. This is most likely caused by the increased V6−O repulsion due to the excess charge mainly localized at V6. The weaker and longer V6−O^{bridge} bonds in $V_2O_5^-$ result in stronger and thus shorter V1−O^{bridge} bonds. Another effect is a smaller degree of pyramidalization at the V6 atom in the anion.

$V_4O_{10}^-$ and V_4O_{10}. $V_4O_{10}^-$ has been detected previously by Rudnyi et al.,[10] who were able to approximately estimate the AEA of V_4O_{10}. A systematic study of possible structures of neutral V_4O_{10} clusters will be given elsewhere.[32] Among several isomers of this composition, the tetrahedral cage is by far the most stable structure. It is analogous to the well-known tetraphosphorus decaoxide molecule and has exact T_d symmetry (Figure 5a). The formation energy of V_4O_{10} from two V_2O_5 fragments is −630.4 (B3LYP) and −606.5 kJ/mol (BP86). The high stability of cage structures of $(V_2O_5)_n$ clusters with $n = 2-12$ is discussed in ref.[32]

The LUMO of V_4O_{10} is a degenerate orbital of *e* symmetry, which consists mainly of suitable linear combinations of *d*-orbitals of vanadium atoms. Therefore, addition of an extra electron to the T_d structure leads to a degenerate ^2E electronic state of the $V_4O_{10}^-$ ion, which undergoes a Jahn−Teller distortion to form a D_{2d} structure. In the D_{2d} structure, $^2A_1$ and $^2B_1$ states result from splitting of the symmetric ^2E state. Both B3LYP and BP86 functionals yield $^2B_1$ as the ground state. However, the $^2A_1-{}^2B_1$ gap is only 0.002 eV (B3LYP) and 0.003 eV (BP86). Because the deviation of the D_{2d} structure from T_d symmetry is also very small, the Jahn−Teller effect is rather weak. The singly occupied b_1 orbital is delocalized over all four metal atoms and has virtually no contribution from oxygen atoms. An important difference between the anionic and the neutral structure is that the V−$O^{terminal}$ bonds are longer in the ion. The same effect is observed in $V_2O_5^-$ (vide supra).

$V_4O_{11}^-$ and V_4O_{11}. In the mass spectra of vanadium vapor in the presence of oxygen, $V_4O_{11}^-$ occurs as a very intensive peak[14] and therefore deserves special attention within the present study. A V_4O_{11} structure can be generated from V_4O_{10} by the addition of another oxygen atom to form of a peroxo complex with a terminally (η^2) coordinated O_2 ligand. The corresponding cage structure is shown in Figure 5b. The peroxo ligand is oriented perpendicularly to one of the V−O−V planes, and the anion has C_s symmetry. Another possible C_s structure with in-plane orientation of the peroxo ligand is a transition structure and lies 9.2 kJ/mol (BP86) above the minimum structure. Thus, the internal rotation is relatively easy. Geometry optimization without symmetry constraints leads to the same structure.

The electronic state for the minimum structure is $^2A'$. The unpaired electron occupies an MO that is delocalized over *d*-orbitals of all four metal atoms and has virtually no contribution from any oxygen atom. It can be rationalized by the fact that the neutral peroxo complex V_4O_{11}, like V_4O_{10}, has the d^0 configuration for all the vanadium atoms. Thus, the extra electron occupies an orbital that is a symmetric combination of the *d*-orbitals of four vanadium atoms (a'). The possibility of a broken-symmetry solution for the wave function of $V_4O_{11}^-$, with the unpaired electron essentially localized on one or two vanadium atoms was also considered. Such a solution cannot be obtained by a conventional SCF procedure, because the starting orbitals, generated either from the core Hamiltonian or from the extended Hückel guess, are symmetric. However, even when started from a broken symmetry solution generated for a modified system, e.g., the isoelectronic $V_3MnO_{11}^+$ ion, the SCF procedure for the original $V_4O_{11}^-$ always converged to the same symmetric solution obtained before. Thus, we conclude that there is no broken-symmetry solution for $V_4O_{11}^-$. The second highest orbital of $V_4O_{11}^-$, a'', has large contributions from all four metal atoms and from the π_g^* orbital of the peroxo ligand. For the V−O_2 bond, this a'' orbital is antibonding. Consequently, a $^2A''$ state is the second lowest state of $V_4O_{11}^-$. The gap between the $^2A'$ and $^2A''$ states is 0.31 eV (B3LYP) and 0.23 eV (BP86).

In the $^2A'$ ground state, the V−O^{peroxo} bonds are relatively short, whereas, correspondingly, the O−O bonds are long (about 1.45 Å). This indicates that the O_2 ligand is strongly bound to the metal. The corresponding neutral molecule, V_4O_{11}, has a similar structure (Figure 5). A small difference is that in this case the in-plane orientation of the O_2 ligand is more favorable, but, again, the energy difference to the perpendicular orientation is small.

4.2. Anions with an Empty Vanadium d-Shell. VO_3^- and VO_3. The charged VO_3^- species has d^0 orbital occupation and, formally, corresponds to the vanadium(V) oxidation state. Therefore, by simple VSEPR considerations, VO_3^- is expected to have a planar D_{3h} structure and a closed-shell singlet $^1A_1'$ ground state. Indeed, our DF calculations confirmed that this configuration is a minimum on the potential energy surface.

The structure of the neutral VO_3 is more complicated. Because the HOMO of the anion is an a_2' orbital, which consists purely of oxygen in-plane orbitals and lies substantially higher (by 0.6 eV) than other orbitals, the neutral species should have a $^2A_2'$ ground state at the structure of the anion. Indeed, both B3LYP and BP86 calculations of the neutral VO_3 at the fixed anion structure give $^2A_2'$ as the ground state. Optimization of the VO_3 structure when constrained to D_{3h} still yields the $^2A_2'$ ground state. The resulting V−O bond length is almost identical to that in the corresponding anion, because the electron is removed from a nonbonding oxygen orbital.

However, CAS SCF calculations[13] showed that the energetically most stable configuration of neutral VO_3 is a *distorted*, slightly nonplanar triangle of C_s symmetry, with only two equivalent V−O bonds. The authors argue that this structure results from the degenerate $^2E'$ state of the symmetric VO_3 (D_{3h}) which undergoes a Jahn−Teller splitting into $^2A_1$ and $^2B_2$ states (C_{2v} symmetry). The latter is the ground state. In complete agreement with these data, our geometry optimization yields a nonplanar C_s structure with two long and one short V−O bonds when the B3LYP functional is applied, whereas the BP86 gives a C_{3v} structure with all V−O distances equal. The deviation from planarity is substantial. The sum of the O−V−O angles is 332° both functionals. The unpaired electron occupies an a_2

SCHEME 3

SOMO of VO_3

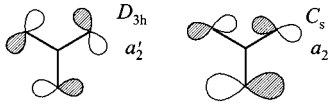

orbital, which consists of oxygen *p*-orbitals. This low-symmetry structure is 19.3 (B3LYP) or 18.9 kJ/mol (BP86) more stable than the D_{3h} structure ($^2A_2'$). In view of the nondegenerate nature of the VO_3 (D_{3h}) ground state ($^2A_2'$), the distortion should not be ascribed to a conventional first-order Jahn−Teller effect, because it could only originate from a $^2E'$ state, which is not the ground state of the symmetric VO_3. It seems to be more appropriate to consider this phenomenon as a second-order Jahn−Teller distortion. The qualitative similarity between the a_2 orbital of the distorted system and the a_2' orbital of the D_{3h} system indicates that the former correlates with the latter rather than with the degenerate e' orbital. In addition, the first-order Jahn−Teller effect cannot explain the nonplanarity of the molecule, because degeneracy is lifted by $D_{3h} \rightarrow C_{2v}$ distortion, but not by $D_{3h} \rightarrow C_{3v}$ distortion. The nature of the distortion is related to the nodal properties of the a_2' orbital. Though *non*-bonding with respect to the V−O bond, it is *anti*-bonding with regard to the O−O interactions (Scheme 3).

Therefore, removal of one electron from this orbital facilitates the oxygen atoms coming closer to each other, thus leading to the pyramidalization of the molecule. In the distorted VO_3 oxygen atoms are separated by about 2.7 Å, whereas in the planar structure the O···O distances are 2.9 Å. A sharp electron detachment peak in the photoelectron spectrum of VO_3^- was interpreted as an indication of the similarity of the of VO_3 and VO_3^- structures.[12] It was argued that the anion should also be a distorted species and have a symmetry lower than D_{3h}. This is contradicted by both our calculations (vide supra) and Hartree−Fock results obtained before.[63]

$V_2O_6^-$ and V_2O_6. Structure predictions for V_2O_6 can be based on the following observations: (a) V_2O_6 can be made up of two VO_3 units, (b) the most stable structure of the neutral V_2O_5 is a doubly bridged $O_2V-(O)_2-V(O)$ configuration with one tri- and one tetracoordinated metal atoms (vide supra); (c) in small and middle-size closed-shell $(V_2O_5)_n$ clusters, vanadium atoms tend to be tetrahedrally coordinated.[32] This consideration leads to the $O_2V-(O)_2-VO_2$ structure (Figure 2), which resembles, for instance, the V_2O_6 fragment in the nonstoichiometric silver vanadate Ag_xVO_3.[64] Although V_2O_6 does not contain peroxo ligands, it certainly belongs to the "oxygen-excessive" species (formal vanadium oxidation state is 6). According to the calculations, such a doubly bridged structure of D_{2h} symmetry is a minimum on the PES. The $V-O^{terminal}$ bonds (about 1.65 Å) are considerably shorter than the $V-O^{bridge}$ bonds.

The doublet ground state of the corresponding anion, $V_2O_6^-$, is $^2B_{1u}$. The singly occupied b_{1u} MO is delocalized over oxygen atoms, with larger contribution from the 2*p* orbitals of the terminal oxo ligands (Scheme 4).

In complete agreement with this, the population analysis shows large spin density on the four terminal O atoms and a smaller spin density at bridging oxygens. As expected, in the neutral V_2O_6 this orbital corresponds to the LUMO. From the structural viewpoint, the $V_2O_6^-$ ion is very similar to the neutral molecule.

Geometrical configurations other than the doubly bridged structure were also considered for $V_2O_6^-$, for example, a singly bridged asymmetric $O_3V-O-VO_2$ cluster, with one tetra- and one tri-coordinated vanadium. However, no local minimum on the potential energy surface corresponding to the latter structure could be located. The optimization finally led to the doubly bridged structure described above.

SCHEME 4

SOMO b_{1u} of $V_2O_6^-$

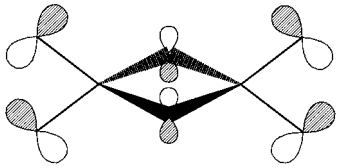

SCHEME 5

HOMO b_2 of $V_3O_8^-$

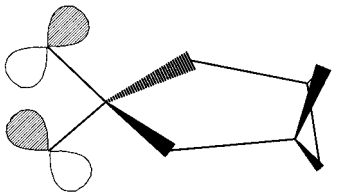

$V_3O_8^-$ and V_3O_8. $V_3O_8^-$ is among the bigger clusters detected in the mass spectra of vanadium vapor in the presence of oxygen.[14] The $V_3O_8^-$ ion is a closed-shell species with vanadium in the oxidation state 5. In view of the trend of vanadium(V) atoms to adopt tetrahedral coordination in clusters,[32] two different structures are worth considering: a chain structure with a linear arrangement of the vanadium atoms connected by double oxygen bridges, and a cyclic structure with one double bridge and two single bridges (Figure 4). Both structures may be considered a "homologous" extension of the $V_2O_6^-$ anion by a VO_2 unit. In the chain structure, a VO_2 unit is added to two terminal oxygen atoms belonging to the same V center, whereas in the ring structure, a VO_2 unit is added to two terminal oxygen atoms belonging to different V centers.

According to the DF calculation, both configurations are minima on the potential energy surface. The cyclic structure with C_{2v} symmetry is 43.9 and 44.3 kJ/mol (B3LYP and BP86, respectively) more stable than the chain with D_{2d} symmetry. Similarly to $V_2O_6^-$ and $V_2O_7^-$, there are large differences between $V-O^{terminal}$ (about 1.6 Å) and $V-O^{bridge}$ (1.7 Å to 1.9 Å) bond lengths. Interestingly, the single oxygen bridges are strongly asymmetric.

The HOMO of $V_3O_8^-$ is a b_2 orbital. It is located almost entirely at the terminal oxygens O2 and O8 (Scheme 5). As expected, the ground state of the corresponding neutral molecule, V_3O_8, at the anion geometry is $^2B_2$. The second lowest state, $^2B_1$, is 0.71 eV (B3LYP) or 0.51 eV (BP86) less stable.

4.3. Anions with Peroxo Ligand. VO_4^- and VO_4. Oxygen-rich species such as VO_4 certainly belong to peroxo complexes. Thus, both VO_4 and the corresponding anion are expected to possess two oxygen atoms connected to each other. Formally, VO_4^- can be formed from V^{5+}, two O^{2-}, and one O_2^{2-}, all of which are closed-shell species. Therefore, VO_4^- should also be a closed-shell system. As expected, the optimized structure of VO_4^- corresponds to the $V(O)_2(O_2)^-$ formula. The O−O distance of about 1.5 Å is typical of a single bond in peroxides. The peroxo ligand is perpendicular to the O−V−O plane, and the metal atom has a distorted tetrahedral environment. The $V-O^{peroxo}$ bonds are much longer compared to the $V-O^{oxo}$ bonds, which are very close to those in VO_3^-. The HOMO of

SCHEME 6

SOMO a_2 of VO_4

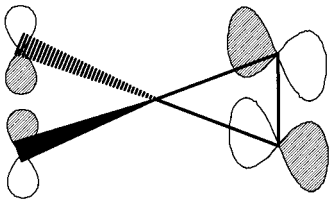

VO_4^- has a_2 symmetry (Scheme 6) and is mainly the π_g* orbital of the peroxo ligand.

Therefore, removing one electron from VO_4^- should lead to an $^2A_2$ ground state of VO_4. Because the electron leaves the antibonding O−O orbital, the O−O bond in the neutral species should be stronger than in VO_4^-. The DF calculations confirm this assumption. Both for the fixed and for the optimized structures of the anion, the $^2A_2$ state is substantially lower than the others. At the minimum structure, the O−O bond shortens by more than 0.1 Å and adopts an essentially double-bond character (Figure 1). At the same time, the $V-O^{peroxo}$ bonds elongate drastically, indicating a quite weak $V-O_2$ bond. As a consequence, the $V-O^{oxo}$ bond lengths decrease and become almost equal to those in VO_2. These findings are consistent with the matrix infrared studies.[61,65] However, an IR study[65] reached the conclusion that in the neutral VO_4, the O_2 ligand has a η^1-type bond to the metal atom, such that a superoxo σ-O_2 ligand emerges. Our calculations do not support this conclusion because both functionals, BP86 and B3LYP, gives two identical $V-O_2$ bonds (η^2 coordination). Our calculated harmonic frequencies at 508 and 513 cm^{-1} ($V-O_2$ asymmetric and symmetric stretching), at 1019 and 1033 cm^{-1} (V−O symmetric and asymmetric stretching), and at 1135 cm^{-1} (O−O stretching) are comparable to observed IR bands of VO_4 in solid argon:[65] 556 (557, supposedly at another site of the matrix), 974 (967), 1122 (or 1127 cm^{-1}).

$V_2O_7^-$ and V_2O_7. The structure of the $V_2O_7^-$ ion can be derived from that of $V_2O_6^-$ by substituting an O atom by a peroxo ligand. Because for $V_2O_6^-$ the doubly bridged structure is the most stable one, two different structures are possible (Figure 3): $O_2V-(O)_2-V(O)(O_2)^-$ with a terminal peroxo ligand, and $O_2V-(O)(O_2)-V(O)_2^-$ with bridging peroxo ligand. The former structure is 57.6 kJ/mol more stable than the latter (BP86). In the most favorable conformation, the anion has C_s symmetry (A'' state) with the O_2 ligand oriented perpendicular to the mirror plane. The singly occupied orbital is delocalized over all the oxygen atoms, but has larger contributions on the bridging atoms than on terminal or peroxo ones. The peroxo ligand contributes to this orbital by its π_g* orbital.

Short O−O bonds and very long $V-O^{peroxide}$ bonds (more than 2 Å) indicate a relatively weak metal-peroxide interaction. As a result, two $V-O^{bridge}$ distances (V1−O4 and V6−O4) are very different. Another C_s conformation with an in-plane oriented O_2 ligand (A' state) corresponds to a transition state and is 54.3 kJ/mol higher in energy (BP86).

The less stable structure with a bridging peroxo ligand contains a planar V−O−V−O−O ring. The O−O bonds are rather short, and the $V-O^{peroxo}$ distances are extremely long. As a consequence of the weak $V-O^{peroxo}$ bonds, the $V-O^{terminal}$ bonds are stronger and shorter than in $V_2O_6^-$. The electronic ground state for the $O_2V-(O)(O_2)-V(O)_2$ anion is $^2A_2$. The a_2 SOMO consists chiefly of *p*-orbitals of four terminal oxygens, and the orbitals of the peroxo ligand contribute only insignificantly.

The structure of the neutral closed-shell V_2O_7 molecule is very similar to the respective anion (Figure 3). Because one electron of $V_2O_7^-$ is removed from a mainly nonbonding orbital, the bonding pattern is not significantly changed. A slightly shorter O−O bond and a little longer $V-O^{peroxide}$ bond are due to the small contribution of the antibonding O−O orbital to the SOMO of the anion.

4.4. Adiabatic Electron Affinities and Vertical Electron Detachment Energies. To evaluate the electron binding to the anions, we calculated their vertical electron detachment energies (VDE) as well as the adiabatic electron affinities (AEA) of the corresponding neutral species. Tab. 2 shows the results. Because diffuse functions usually stabilize anions, detachment energies are expected to become larger when such functions are added. We augmented the TZVP basis set on oxygen by additional diffuse *s*- and *p*-type function with $\zeta = 0.0845$[66] (This basis set is labeled TZVP+) and performed VDE and AEA calculations using structures optimized with the TZVP basis set. They are also shown in Table 2. For mono-nuclear ions that have a relatively low VDE such as VO_2^- and VO_3^-, diffuse functions increase the calculated VDE by about 0.2 eV (Tab. 2). For species with a higher VDE, only a minor change (at most 0.1 eV) is found. Diffuse functions play a smaller role if the excess electron is strongly bound.

A few experimental results are available for comparison. VO (d^3 configuration, $^3\Sigma^-$ state) exhibits a relatively low AEA (about 0.8 eV) both with B3LYP and BP86 functionals. This is lower than the experimental value of 1.23 eV. The B3LYP result of Gutsev et al.,[60] 1.09 eV, is closer to the observed one probably because a larger basis set is used on V. They also found a positive AEA for the $^5\Pi$ state of VO^- whereas our basis set predicts that it is unstable with respect to the $^4\Sigma^-$ state of the neutral molecule.

VO_2 (d^2 configuration) is predicted to have a higher AEA (1.7−1.9 eV) than VO. Compared to the experimental value of 2.03 eV[12] and 2.31 ± 0.2 eV,[10] the calculated result is also underestimated. The VDE of VO_3^- calculated as a difference between the anionic $^1A_1'$ and neutral $^2A_2'$ states is between 4.22 (BP86) and 4.45 eV (B3LYP). The adiabatic electron affinity of VO_3 was calculated using the nonplanar neutral VO_3 structure. Compared to the experimental value of 4.36 eV,[12] the BP86 result (4.03 eV) is somewhat too small, but the B3LYP result (4.26 eV) is in very good agreement. V_4O_{10} is the only polynuclear vanadium oxide cluster known to us whose electron affinity has been experimentally estimated.[10] Our calculations using both B3LYP and BP86 functionals give values that are within the experimental error limits (4.16 ± 0.6 eV).

The photoelectron spectrum of VO_4^- shows a very broad electron detachment feature in the range from 3.9 to 4.7 eV,[12] which indicates substantial structure differences between VO_4 and VO_4^-. This is in line with our DF predictions. A crude experimental estimate of the adiabatic electron affinity is 4.0 eV. The DF calculation gives a value of about 3.6 eV (Tab. 2). VDEs are, however, larger than 4 eV. Thus, electron detachment energies do not increase when passing from VO_3^- to VO_4^-. This finding is in accord with previous observation that the electron detachment energy does not increase significantly from CuO_2^- to CuO_6^-.[18]

Comparison of the predicted AEA with the few experimental data available indicates that the calculated values are systematically underestimated by about 0.3 ± 0.2 eV. In all cases, the

TABLE 2: Vertical Electron Detachment Energies (VDE) of $V_xO_y^-$ Ions and Adiabatic Electron Affinities (AEA) of the Corresponding Neutral Species $V_xO_y^-$ in eV[a]

	symmetry	VDE			AEA		
ion	ion/neutral	B3LYP	BP86	exp[c]	B3LYP	BP86	exp[c,d]
VO^-	$C_{\infty v}/C_{\infty v}$						
$^5\Pi \rightarrow {}^4\Sigma^-$		−0.03 (−0.24)	−0.06 (−0.27)		−0.22 (−0.45)	−0.21 (−0.42)	
$^3\Sigma^- \rightarrow {}^4\Sigma^-$		0.86 (0.75)	0.83 (0.72)		0.85 (0.74)	0.83 (0.71)	1.23[c]
VO_2^-	C_{2v}/C_{2v}	1.95 (1.74)	1.85 (1.65)		1.86 (1.63)	1.71 (1.49)	2.03/2.31 ± 0.2[d]
$V_2O_4^-$	D_{2h} (C_{2v})[b]/C_{2v}	3.04 (2.89)	2.95 (2.80)		2.62 (2.47)	2.66 (2.51)	
$V_2O_5^-$	C_s/C_s	4.77 (4.66)	4.18 (4.08)		4.13 (4.02)	3.72 (3.62)	
$V_4O_{10}^-$	D_{2d}/T_d	4.52 (4.49)	4.48 (4.45)		4.45 (4.40)	4.40 (4.37)	4.16 ± 0.6[d]
$V_4O_{11}^-$	C_s/C_s	5.28 (5.25)	4.59 (4.57)		4.65 (4.62)	4.33 (4.20)	
VO_3^-	D_{3h}/C_s	4.45 (4.27)	4.22 (4.04)	~3.8−4.4	4.26 (4.07)	4.03 (3.84)	4.36
$V_2O_6^-$	D_{2h}/D_{2h}	6.80 (6.73)	6.17 (6.10)		6.80 (6.72)	6.16(6.09)	
$V_3O_8^-$	C_{2v}/C_{2v}	6.14 (6.08)	5.91 (5.85)		5.66 (5.60)	5.64 (5.59)	
VO_4^-	C_{2v}/C_{2v}	4.29 (4.17)	4.18 (4.06)	~3.9−4.7	3.57 (3.45)	3.59 (3.47)	4.0
$V_2O_7^-$	C_s/C_s	7.11 (7.05)	6.29 (6.23)		6.87 (6.82)	6.17 (6.11)	

[a] TZVP basis set augmented with diffuse functions. Values in parentheses: TZVP without diffuse functions. [b] B3LYP (BP86) prediction. [c] Ref 12 [d] Ref 10

SCHEME 7

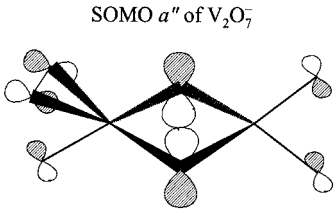

BP86 functional yields smaller AEA than the B3LYP functional. Thus, B3LYP predictions are somewhat more reliable. It should be noted, however, that all experimentally known data apply to mononuclear species. Despite the discrepancy concerning the determination of the electronic ground state of V_2O_4, the B3LYP and BP86 predictions of the VDE of $V_2O_4^-$ and of the AEA of V_2O_4, agree within 0.09 and 0.04 eV, respectively.

The calculated VDE and AEA values strongly vary with the type and structure of the anion. Two different types can be distinguished:

(a) Anions with partially occupied vanadium *d*-shells: VO^-, VO_2^-, $V_2O_4^-$, $V_2O_5^-$, $V_4O_{10}^-$, and $V_4O_{11}^-$.

(b) Anions with an O-2*p* SOMO or HOMO delocalized over the O atoms: VO_3^-, $V_2O_6^-$, $V_3O_8^-$ (Schemes 3−5). The $V_2O_7^-$ anion also belongs in this category because there is only a small admixture of the antibonding π^* orbital of the peroxo ligand to the delocalized O-2*p* orbital (Scheme 7).

The VO_4^- anion is a special case, because the antibonding π^* orbital of the peroxo ligand dominates the HOMO.

Figure 6 shows that the VDE of the anions with partially occupied *d*-shell, group (a), increase with decreasing average occupation of the *d*-shell. The average formal *d*-shell occupation *n* is evaluated as the ratio of the total formal number of *d*-electrons to the number of V atoms. Even VO^- follows this trend, but this point is off the line. The correlation found renders a prediction of VDE for $V_xO_y^-$ anions of type (a) possible. The limiting value for large clusters with one *d*-electron on one vanadium only ($n = 0$) is about 5.8 eV (BP86 functional), whereas the opposite limit value for clusters having one *d*-electron on every vanadium atom ($n = 1$) is about 3.3 eV.

The VDE of anions with a delocalized O-2*p* SOMO fall into the range between 4.2 (VO_3^-) and 6.3 eV ($V_2O_7^-$). The VDE of $V_3O_8^-$ (5.9 eV) is smaller than that of $V_2O_6^-$ (6.2 eV). This is contrary to the expectation that in a larger closed-shell anion the excess electron is more strongly bound than in a smaller open-shell system. The reason is the different degree of delocalization. Only two terminal O atoms contribute to the HOMO of $V_3O_8^-$ (Scheme 5), whereas the SOMO in $V_2O_6^-$ is distributed over six oxygen atoms (Scheme 4). The energy of a molecular orbital does not only depend on the number of atoms *N* over which it is delocalized but also on the number of nodal planes *m*. Hence, the VDE is expected to increase with decreasing ratio $p = m/N$. Figure 6 shows that this is indeed the case. Except for the special case of the mononuclear anion VO_3^-, *p* is between 0.5 and 0.0. (For simplicity, we count the nodal planes given by symmetry only.) From the plot in Figure 6, we conclude that for all $V_xO_y^-$ anions with an O−2*p* SOMO ($x \neq 1$), the VDE are between 6 and 7.5 eV.

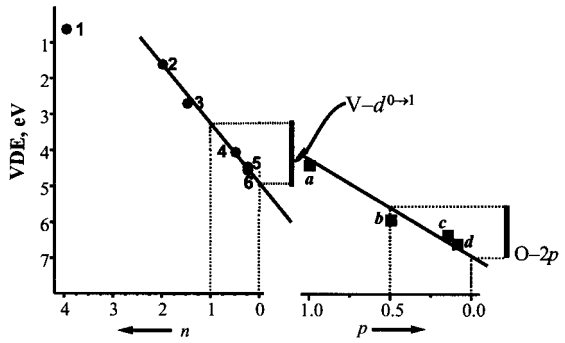

Figure 6. Vertical detachment energies of $V_xO_y^-$ ions with partly occupied vanadium *d*-shells, VO^- (*1*), VO_2^- (*2*), $V_2O_4^-$ (*3*), $V_2O_5^-$ (*4*), $V_4O_{10}^-$ (*5*) and $V_4O_{11}^-$ (*6*) at BP86/TZVP+ level versus average formal *d* occupation *n* (left-hand part, **circles**) and that of ions with empty vanadium *d*-shells, VO_3^- (*a*), $V_3O_8^-$ (*b*), $V_2O_6^-$ (*c*), and $V_2O_7^-$ (*d*) versus $p = m/N$ (right-hand part, **squares**) (*N* is the number of atoms, *m* is the number of nodal planes of the HOMO).

4.5. Reaction Energies. Although electron detachment energies of the anions indicate their stability with respect to the loss of an electron, the energies of some chemical reactions can hint on their chemical stability. Because under experimental conditions the $V_xO_y^-$ ions are generated from vanadium vapor and oxygen,[14] most important are energies of oxygen uptake and, in the case of bigger ions, possibly also energies of formation from smaller clusters. Table 3 shows selected reaction energies. Energies for other possible reactions can be calculated from the total energy tables (Tables 4 and 5). The relative stability of clusters of the composition $(V_2O_5)_n$ with $n = 1-12$ is discussed in ref.[32] The formation of larger species from smaller ones is exothermic because coordinatively saturated species with a larger number of V−Oσ-bonds are formed from unsaturated ones. For the reaction

TABLE 3: Selected Reaction Energies (TZVP basis set)

reaction	reaction energy ΔE, kJ/mol	
	B3LYP	BP86
$VO_2 + VO_2 \rightarrow V_2O_4$	−441.9	402.3
$VO_2 + VO_3 \rightarrow V_2O_5$	−510.0	−532.1
$VO_3 + VO_3 \rightarrow V_2O_6$	−230.4	287.5
$V_2O_5 + VO_3 \rightarrow V_3O_8$	−465.0	−438.0
$VO_2 + {}^1/_2\,O_2 \rightarrow VO_3$	−126.0	−190.5
$VO_3^- + {}^1/_2O_2 \rightarrow VO_4^-$	−50.3	−60.9
$VO_2^- + {}^1/_2O_2 \rightarrow VO_3^-$	−355.6	−393.9
$VO^- + {}^1/_2O_2 \rightarrow VO_2^-$	−458.0	−496.7
$V_4O_{10}^- + {}^1/_2O_2 \rightarrow V_4O_{11}^-$	−87.4	−80.9
$V_2O_6^- + {}^1/_2O_2 \rightarrow V_2O_7^-$	−65.3	−34.4
$V_2O_5^- + {}^1/_2O_2 \rightarrow V_2O_6^-$	−107.0	−184.8
$V_2O_4^- + {}^1/_2O_2 \rightarrow V_2O_5^-$	−398.1	−429.4
$VO_2^- + VO_2 \rightarrow V_2O_4^-$	−462.2	−474.5
$V_2O_6^- + VO_2 \rightarrow V_3O_8^-$	−637.0	−634.4
$V_3O_8^- + VO_2 \rightarrow V_4O_{10}^-$	−554.3	−559.8
$V_3O_8^- + VO_3 \rightarrow V_4O_{11}^-$	−346.4	−311.4
$V_2O_5^- + VO_3 \rightarrow V_3O_8^-$	−1005.6	−977.5
$VO_2^- + VO_3 \rightarrow V_2O_5^-$	−346.7	−364.6
$V_2O_4 + O^- \rightarrow V_2O_5^-$	−167.4	−253.2
$V_2O_5 + O^- \rightarrow V_2O_6^-$	−651.6	−706.1
$V_2O_6 + O^- \rightarrow V_2O_7^-$	−870.5	−794.6
$V_4O_{10} + O^- \rightarrow V_4O_{11}^-$	−494.5	−513.2
$VO_3 + O^- \rightarrow VO_4^-$	−600.1	−604.3
$VO_2 + O^- \rightarrow VO_3^-$	−675.9	−733.9
$VO + O^- \rightarrow VO_2^-$	−571.9	−628.9

TABLE 4: Absolute Energies of Vanadium Oxide Anions

anion	absolute energy (*Hartree*)	
	B3LYP/TZVP	BP86/TZVP
VO^- ($^5\Pi$)	−1019.103 53	−1019.375 78
($^3\Sigma^-$)	−1019.146 93	−1019.417 26
VO_2^- ($^3B_2$)	−1094.439 02	−1094.765 93
($^1A_1$)	−1094.416 70	−1094.753 89
VO_3^- ($^1A_1'$)	−1169.735 52	−1170.116 92
VO_4^- ($^1A_1$)	−1244.915 73	−1245.341 07
$V_2O_4^-$ ($^4B_{2g}/^4B_1$)	−2189.017 01	−2189.668 94
($^2B_2$)	−2188.991 86	−2189.648 79
($^2A_2$)	−2188.979 71	−2189.656 49
$V_2O_5^-$ ($^2A'$)	−2264.304 57	−2265.013 32
($^2A''$)	−2264.281 85	−2264.983 61
$V_2O_6^-$ ($^2B_{1u}$)	−2339.506 39	−2340.284 65
($^2B_{2u}$)	−2339.451 51	−2340.231 77
$V_2O_7^-$ ($^2A''$)	−2414.692 34	−2415.498 73
($^2A_2$)	−2414.671 34	−2415.476 79
$V_3O_8^-$ ring ($^1A_1$)	−3434.125 79	−3435.228 40
chain ($^1A_1$)	−3434.109 07	−3435.211 52
$V_4O_{10}^-$ ($^2B_1$)	−4528.715 91	−4530.152 64
($^2A_1$)	−4528.715 83	−4530.152 51
$V_4O_{11}^-$ ($^2A'$)	−4603.843 58	−4605.322 64
($^2A''$)	−4603.832 28	−4605.314 17
O^- (^2P)	−75.101 29	−75.135 26

$$2VO_2 \rightarrow V_2O_4$$

comparison with thermochemical data is possible. If heats of formation for both species are taken from ref 44, an estimate of -530 ± 51 kJ/mol is obtained, whereas a value of -413 ± 23 is obtained when the heat of formation of VO_2 is taken from ref 10. The B3LYP prediction of the reaction energy (−442 kJ/mol, Table 3) is bracketed by the two experimental estimates and the BP86 result (−402 kJ/mol) is close to the smaller estimate. Hence, despite their large uncertainty, the few thermochemical data available support the results of DF calculations.

The formation energies of $V_2O_4^-$, $V_2O_5^-$, $V_2O_6^-$, $V_3O_8^-$, $V_4O_{10}^-$, and $V_4O_{11}^-$ from smaller clusters show that the polynuclear anions are relatively stable. Relying on the calculated values, one can expect that $V_3O_8^-$ should be a very stable species.

TABLE 5: Absolute Energies of Neutral Vanadium Oxide Clusters

neutral	absolute energy (*Hartree*)	
	B3LYP/TZVP	BP86/TZVP
VO ($^4\Sigma^-$)	−1019.119 89	−1019.391 13
VO_2 ($^2A_1$)	−1094.379 01	−1094.711 01
($^2B_2$)	−1094.376 79	−1094.702 13
VO_3 ($^2A''$)	−1169.585 86	−1169.975 65
VO_4 ($^2A_2$)	−1244.789 07	−1245.213 68
V_2O_4 ($^3B_2$)	−2188.926 33	−2189.575 24
($^3A_2$)	−2188.905 11	−2189.576 65
($^1A_2$)[a]	−2188.889 62	−2189.562 39
($^1B_2$)[a]	−2189.803 92	−2189.513 89
V_2O_5 ($^1A'$)	−2264.156 92	−2264.880 45
V_2O_6 ($^1A_{1g}$)	−2339.259 48	−2340.060 81
V_2O_7 ($^1A'$)	−2414.441 89	−2415.274 32
V_3O_8 ($^2B_2$)	−3433.919 90	−3435.022 94
V_4O_{10} ($^1A_1$)	−4528.553 96	−4529.991 92
V_4O_{11} ($^1A'$)	−4603.673 90	−4605.164 68
O_2 ($^3\Sigma^-$)	−150.322 13	−150.401 93
O (^3P)	−75.065 60	−75.091 49

[a] Single-point energy evaluated by broken-symmetry appoach.

The oxygen uptake energies for the mononuclear ions VO_y^- indicate that the formation of a peroxo group is not as favorable as previous oxygen uptake steps. Also, oxidation of $V_2O_6^-$ to the binuclear peroxo complex $V_2O_7^-$ as well as of $V_4O_{10}^-$ to $V_4O_{11}^-$ is much less favorable than oxidation of $V_2O_4^-$ to $V_2O_5^-$ and of $V_2O_5^-$ to $V_2O_6^-$. These results are in agreement with the presumably weak metal-peroxide bonds. The overall trend is that oxygen uptake energies decrease with increasing oxygen-to-vanadium ratio. Formation of oxygen-richer anions from neutral species and an oxide ion is a rather favorable reaction. The VO_2^- dissociation energy with respect to the O^- detachment can be compared with the experimental data of Rudnyi et al.[10] The experimental value of 630 ± 19 kJ/mol agrees satisfactory with the calculated B3LYP result (572 kJ/mol) and virtually coincides with the BP86 (629 kJ/mol) one.

5. Summary

The structures of vanadium oxide anions $V_xO_y^-$ and the respective neutral species have been determined by DF calculations using the B3LYP and BP86 functionals. Comparison with experimental results and results of high-level ab initio methods available for mononuclear $VO_x^{-/0}$ species shows a very good performance of DF calculations. Bond distances are reproduced within 0.03 Å. Calculated vibrational frequencies of VO_2 and VO_4^- can be assigned to bands observed for these species in the matrix.

For all the species studied, the following average distances are predicted for the different types of V−O bonds (B3LYP/BP86): terminal 1.63/1.65 Å, bridging 1.85/1.84 Å, $V-O^{peroxo}$ 1.94/1.94 Å. In the peroxo ligands the O−O bond distance is 1.40/1.41 Å. Of the two functionals, BP86 should be preferred to B3LYP for structure determinations, because it yields structures of the same quality and is much faster when codes are used that take advantage of the RI-method[30] such as TURBOMOLE.[31]

Experimental atomization energies and electronic excitation energies in the anions are better reproduced by BP86 than by B3LYP results. The adiabatic electron affinities (AEA) of mononuclear species are slightly underestimated by both functionals. In this case B3LYP performs slightly better (deviation 0.26 eV) than BP86 (deviation 0.36 eV). In general, BP86 results are smaller than B3LYP results both for AEA (by 0.0 to 0.6 eV) and VDE (by 0.1−0.8 eV). Unfortunately, only one VDE has been experimentally estimated for a poly-nuclear $V_xO_y^-$ anion.

Our predictions for the VDEs of $V_xO_y^-$ anions use B3LYP values. Apart from the mono-nuclear species that are special, two types of anions can be distinguished. (a) For species with partially occupied *d*-shells (mixed valence V^{IV}/V^{V} anions), ionization takes place from the vanadium *d*-orbitals and the VDE is expected to vary between 4.0 (V^{IV} only) and 5.8 eV (almost only V^{V}). (b) For anions with formal V oxidation state +5 or larger, ionization is out of an O-2*p* orbital which is more or less delocalized over the oxygen atoms. The VDE is predicted between 6.0 and 7.5 eV. To correct for systematic errors an increment of 0.25 eV may be added to these B3LYP predictions. The VDEs of anions with peroxo-groups do not show any peculiarities. They belong to either of the two groups mentioned.

Energies for oxygen uptake decrease with increasing oxygen-to-vanadium ratio. They are particularly low when a peroxo group is formed. Formation of larger species from smaller ones is energetically favorable. In this respect, $V_3O_8^-$ appears to be particularly stable among the anions examined in the present study.

Acknowledgment. We are grateful to Professor K. Rademann and Dr. A. Pramann for fruitful discussions as well as for making their results available prior to publication. This work has been supported by the Deutsche Forschungsgemeinschaft within the Sonderforschungsbereich 546, by the Max-Planck-Gesellschaft, and by the Fonds der chemischen Industrie. The computational power provided by the Konrad-Zuse-Zentrum für Informationtechnik Berlin is also appreciated.

References and Notes

(1) Kung, H. H. *Adv. Catal.* **1989**, *40*, 1.
(2) Haggin, J. *Chem. Eng. News* **1995**, *73*, 20.
(3) Topsøe, N.-Y. *Science* **1994**, *265*, 1217.
(4) Bell, R. C.; Zemski, K. A.; Kerns, K. P.; Deng, H. T.; Castleman, A. W., Jr. *J. Phys. Chem. A* **1998**, *102*, 1733.
(5) Kooi, S. E.; Castleman, A. W., Jr. *J. Phys. Chem. A* **1999**, *103*, 5671.
(6) Bell, R. C.; Zemski, K. A.; Castleman, A. W., Jr. *J. Phys. Chem. A* **1999**, *103*, 2992.
(7) Bell, R. C.; Zemski, K. A.; Castleman, A. W., Jr. *J. Phys. Chem. A* **1999**, *103*, 1585.
(8) Harvey, J.; Diefenbach, M.; Schröder, D.; Schwarz, H. *Int. J. Mass Spectrom.* **1999**, *182/183*, 85.
(9) Foltin, M.; Stueber, G. J.; Bernstein, E. R. *J. Chem. Phys.* **1999**, *111*, 9577.
(10) Rudnyi, E. B.; Kaibicheva, E. A.; Sidorov, L. N. *J. Chem. Thermodyn.* **1993**, *25*, 929.
(11) Dinca, A.; Davis, Th. P.; Fisher, K. J.; Smith, D. R.; Willett, G. D. *Int. J. Mass Spectrom.* **1999**, *182/183*, 73.
(12) Wu, H.; Wang, L.-S. *J. Chem. Phys.* **1998**, *108*, 5310.
(13) Knight, L. B., Jr.; Babb, R.; Ray, M.; Banisaukas, T. J., III.; Russon, L.; Dailey, R. S.; Davidson, E. R. *J. Chem. Phys.* **1996**, *105*, 10 237.
(14) Rademann, K.; Pramann A. private communication; Humboldt-Universität: Berlin, 1999.
(15) Rohmer, M.-M.; Bénard, M.; Blaudeau, J.-P.; Maestre, J.-M.; Poblet, J.-M.; *Coord. Chem. Rev.* **1998**, *178*−*180*, 1019.
(16) Kempf, J.-Y.; Rohmer, M.-M.; Poblet, J.-M.; Bo, C.; Bénard, M. *J. Am. Chem. Soc.* **1992**, *114*, 1136.
(17) Rohmer, M.-M.; Bénard, M. *J. Am. Chem. Soc.* **1994**, *116*, 6959.
(18) Wu, H.; Desai, S. R.; Wang, L. S. *J. Phys. Chem. A* **1997**, *101*, 2103.
(19) Wu, H.; Desai, S. R.; Wang, L. S. *J. Am. Chem. Soc.* **1996**, *118*, 5296.
(20) Desai, S. R.; Wu, H.; Rohfling, C.; Wang, L. S. *J. Chem. Phys.* **1997**, *106*, 1309.
(21) Gutsev, G. L.; Khanna, S. N.; Rao, B. K.; Jena, P. *J. Phys. Chem. A* **1999**, *103*, 5812.
(22) Parr, R. G.; Yang, W. *Density Functional Theory of Atoms and Molecules*; Oxford University Press: New York, 1989.
(23) Becke, A. D. *Phys. Rev. A* **1988**, *38*, 3098.
(24) Lee, C.; Yang, W.; Parr, R. G. *Phys. Rev. B* **1988**, *37*, 785.
(25) Becke, A. D. *J. Chem. Phys.* **1993**, *98*, 5648.
(26) Stephens, P. J.; Devlin, C. F.; Chabalowski, M. J.; Frisch, M. J. *J. Phys. Chem.* **1994**, *98*, 11 623.
(27) Perdew, B. P. *Phys. Rev. B* **1986**, *B33*, 8822.
(28) Koch, W.; Hertwig, R. In *Encyclopedia of Computational Chemistry*; Schleyer, P.v. R., Ed.; John Willey & Sons: Chichester, 1998; vol. 1, 689−700.
(29) Curtiss, L. A.; Redfern, P. C.; Raghavachari, K.; Pople, J. A. *J. Chem. Phys.* **1998**, *109*, 42.
(30) Eichkorn, K.; Treutler, O.; Öhm, H.; Häser, M.; Ahlrichs, R. *Chem. Phys. Lett.* **1995**, *240*, 283.
(31) Ahlrichs, R.; Bär, M.; Häser, M.; Horn, H.; Kölmel, C. M. *Chem. Phys. Lett.* **1989**, *162*, 165; *Program TURBOMOLE*. TURBOMOLE is commercially available from MSI: San Diego, CA.
(32) Vyboishchikov, S. F.; Sauer, J., manuscript in preparation.
(33) Schäfer, A.; Horn, H.; Ahlrichs, R. *J. Chem. Phys.* **1994**, *100*, 5829.
(34) Wachters, A. J. H. *J. Chem. Phys.* **1970**, *52*, 1033.
(35) Noodleman, L. *J. Chem. Phys.* **1981**, *74*, 5737.
(36) Windiks, R.; Sauer, J. *Phys. Chem. Chem. Phys.* **1999**, *1*, 4505.
(37) *Gaussian 94, Revision B.3*, Frisch, M. J.; Trucks, G. W.; Schlegel, H. B.; Gill, P. M. W.; Johnson, B. G.; Robb, M. A.; Cheeseman, J. R.; Keith, T.; Petersson, G. A.; Montgomery, J. A.; Raghavachari, K.; Al-Laham, M. A.; Zakrzewski, V. G.; Ortiz, J. V.; Foresman, J. B.; Peng, C. Y.; Ayala, P. Y.; Chen, W.; Wong, M. W.; Andres, J. L.; Replogle, E. S.; Gomperts, R.; Martin, R. L.; Fox, D. J.; Binkley, J. S.; Defrees, D. J.; Baker, J.; Stewart, J. J. P.; Head-Gordon, M.; Gonzalez, C.; Pople, J. A. Gaussian, Inc.: Pittsburgh, PA, 1995.
(38) Li, J.; Correa de Mello, P.; Jug, K.; *J. Comput. Chem.* **1992**, *13*, 85
(39) Sallans, L.; Lane K.; Squires, R. R.; Freiser, B. S. *J. Am. Chem. Soc.* **1985**, *107*, 4379.
(40) Armentrout, P. B. In *C*−*H Activation*, Liebmann, J., Greenberg, A., Eds.; VCH: New York, 1990.
(41) Elkind, J. L.; Armentrout, P. B. *J. Phys. Chem.* **1985**, *89*, 5626.
(42) Aristov, N.; Armentrout, P. B. *J. Am. Chem. Soc.* **1984**, *106*, 4065.
(43) Pedley, J. B.; Marshall, E. M. *J. Phys. Chem. Ref. Data* **1983**, *12*, 967.
(44) Balducci, G.; Gigli, G.; Guido, M. *J. Chem. Phys.* **1983**, *79*, 5616.
(45) Huber, K. P.; Herzberg, G. *Molecular Spectra and Molecular Structure. IV. Constants of Diatomic Molecules*; Van Nostrand Reinhold: New York, 1979.
(46) Huang, G.; Merer, A. J.; Clouthier, D. J. *J. Mol. Spectrosc.* **1992**, *153*, 32.
(47) Flesch, G. D.; Svec, H. J. *Inorg. Chem.* **1975**, *14*, 1817.
(48) Merer, A. J. *Annu. Rev. Phys. Chem.* **1989**, *40*, 407.
(49) Merer, A. J.; Huang, G.; Cheung, A. S.-C.; Taylor, A. W. *J. Mol. Spectrosc.* **1987**, *125*, 465.
(50) Dyke, J. M.; Gravenor, B. W. J.; Hastings, M. P.; Morris, A. *J. Phys. Chem.* **1985**, *90*, 189.
(51) Cheung, A. S.-C.; Taylor, A. W.; Merer, A. J. *J. Mol. Spectrosc.* **1982**, *92*, 391.
(52) Cheung, A. S.-C.; Hansen, R. C.; Merer, A. J. *J. Mol. Spectrosc.* **1982**, *91*, 165.
(53) Bakalbassis, E. G.; Stiakaki, M.-A. D.; Tsipis, A. C.; Tsipis, C. A. *Chem. Phys.* **1996**, *205*, 389.
(54) Dolg, M.; Wedig, U.; Stoll, H.; Preuss, H. *J. Chem. Phys.* **1987**, *86*, 2123.
(55) Bauschlicher, C. W., Jr.; Maitre, P., S. R. *Theor. Chim. Acta* **1985**, *90*, 189.
(56) Bauschlicher, C. W., Jr.; Langhoff, S. R. *J. Chem. Phys.* **1986**, *85*, 5936.
(57) Broclawik E., In *Modern Density Functional Theory: A Tool for Chemistry*; Seminario, J. M., Politzer, P., Eds.; vol. 2, p 349.
(58) Broclawik, E. *Int. J. Quantum Chem.* **1995**, *56*, 779.
(59) Piechota, J.; Suffczyński, M. *Z. Phys. Chem. (Munich)* **1997**, *200*, 39.
(60) Gutsev, G. L.; Rao, B. K.; Jena, P. *J. Phys. Chem. A*, **2000**, *104*, 5374.
(61) Almond, M. J.; Atkins, R. W. *J. Chem. Soc., Dalton Trans.* **1994**, 835.
(62) Fink, K.; Fink, R.; Staemmler, V. *Inorg. Chem.* **1994**, *33*, 6219.
(63) Ramondo, F.; Bencivenni, L.; Sanna, N.; Cesaro, S. N. *J. Mol. Struct. (THEOCHEM)*, **1992**, *253*, 121.
(64) Rozier, P.; Savariault, J.-M.; Galy, J. *J. Solid State Chem.* **1996**, *122*, 303.
(65) Chertihin, G. V.; Bare, W. D.; Andrews, L. *J. Phys. Chem. A* **1997**, *85*, 5090.
(66) Clark, T.; Chandrasekhar, J.; Schleyer, P.v. R. *J. Comput. Chem.* **1983**, *4*, 294.